Study of jet composition at particle level and its implications for Energy Flow algorithms

December 9, 2004

C. Iglesias
TileCal Group-IFIC(Valencia)
Universidad de Valencia-CSIC
in collaboration with M. Bosman (IFAE, Barcelona)

Abstract: The performance of Energy Flow algorithms will be limited by the overlap of particles. In this note, we study the jet composition (particle densities, PT spectra and nature, etc).
The maximum potential gain in E_T resolution of the Energy Flow algorithm at LHC with the ATLAS detector is estimates taking into account only shower shape effects in a simplified way.
The impact of Underlying event and Minimum bias events at low luminosity has been also considered .
This particle level study should be followed up for full simulation of detector response, to obtain a realist estimate of the energy resolution that can be reached by a study in ATLAS with an Energy Flow approach.

1 Aim of this note

This study is a first step in the exploration of the potential of the Energy Flow algorithm at LHC with the ATLAS detector. The aim of the Energy Flow Algorithm is to make optimal use of the detector information combining the measured of the energy deposition in towers or cells of the calorimeter with the reconstructed tracks in the central detector to improve jet energy resolution and missing transverse energy, E_T^{miss}.

Here we report on a study of the composition of jets composition of jets (particle densities, PT spectra and nature, etc) at particle level as well as the effects of Underlying event and Minimum bias events at low luminosity. These studies have been carried out in order to understand better the environment and the importance of the overlap between charged and neutral particles when doing later full simulation and attacking the hart of the problem of cluster-track association and energy subtraction.

2 Energy Flow Concept

The Energy Flow algorithm was introduced for the first time in the ALEPH[1] detector in 1994-1995, and it was extensively developed in the four experiments at LEP[2]. The reconstruction of individual particles (charged or neutral) in LEP detectors was very difficult because of coarse calorimeter granularity, small magnetic field, lack of longitudinal segmentation, and additional dead material in front of or inside the calorimeter.

Nowadays, the Energy Flow technique has been improved by experiments, such as CDF[3] and D0 (Tevatron, Run II), H1[4], ZEUS[5], TESLA[6] and finally it just starting to study in the general purpose detectors of LHC, CMS[7] and ATLAS[8] (whether in full simulation[9] or fast simulation[10]).

Around 2/3 of the jet energy comes from charged particles (mainly pions and kaons). However classical jet reconstruction algorithms only use calorimeter energy information. The concept of the Energy Flow algorithm is to exploit the measured of charged track momentum instead of energy.

For low momentum charged particles, the tracking error is much smaller than the calorimetric energy error[11]. A simple calculation of the relation between the p_T resolution of the inner detector and the energy resolution of the Hadronic calorimeter of ATLAS can be done. The resolution of the tracking system, in the general case, is managed in ATLAS TDR[12] and is given by the formula:

$$\sigma(\frac{1}{p_T}) = 0.36 \oplus \frac{13}{P_T\sqrt{\sin\theta}} \tag{1}$$

where the track resolution appears in TeV^{-1} and the P_T in GeV. As we are going to study only the central barrel case, we can assume $\eta = 0$ and $sin\theta = 1$, so for this particular case, the relative resolution, $\frac{\sigma(p_T)}{p_T}$, in terms of per cent, %, can be written as follows:

$$\frac{\sigma(P_T)}{P_T} = 0.036\% p_T \oplus 1.3\% \tag{2}$$

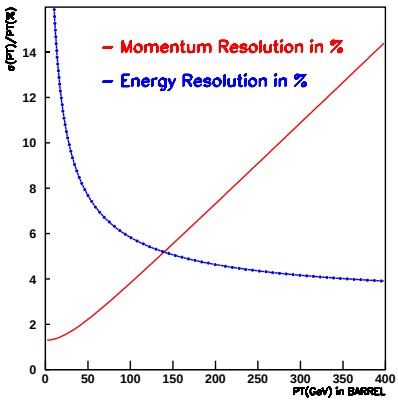

Figure 1: Transverse momentum (P_T) resolution in the Inner Detector versus energy resolution in the Hadronic Calorimeter at $\eta = 0$. The Energy Flow algorithm may improve resolution for p_T values smaller than about 140 GeV, value where both resolutions are equal.

On the other hand, the energy resolution of the hadronic calorimeter in the central barrel area for the case of the jets is given by:

$$\frac{\sigma(E)}{E} = \frac{50\%}{\sqrt{E}} \oplus 3\% \tag{3}$$

So, for one pion of 10 GeV the tracking resolution, 1.3%, is much smaller than the energy resolution, 16%. This behaviour appears for low momentum and it implies that the Energy Flow algorithm is interesting of using for p_T values smaller than 140 GeV, value where both resolutions are equal.

The basic idea of the algorithm is to substitute the random fluctuations of energy in the calorimeter by the well measured charged particle momentum, in order to obtain better resolution in jet energy.

In this analysis we use calorimeter energy resolution for neutral hadrons while we use tracker resolution for charged hadrons. We first localize the expected energy deposit in electromagnetic (EM) and hadronic (HAD) cluster by the charged hadrons in order to remove it and substitute it by the measurement of the momentum.

The use of track momentum improves resolution only if cluster is isolated. Then, if track shares a cluster with neutral particle, the gain in resolution from track will be limited by loss of resolution of the remaining cluster. So, the efficiency of the algorithm is limited by the overlap between neutral and charged particles in the cells of the calorimeter, effects that we will study more in details.

The method is simple but however challenging realized: it requires building the particle ID associated with the track. This starts running into difficulties in high track multiplicity environment and coarse calorimeter granularity: it requires use of advanced clustering algorithm capable of efficient isolation of the individual showers, together with an energy deposition model.

3 Parameterization of the energy in Atlfast

This study is performed with the particle level fast simulation package developed by the ATLAS computing community, named Atlfast[13][14]. This package is by definition too simplistic and limits the validity of the final results, but they can be used as input to full simulation studies.

In Atlfast there is no detailed simulation of the particle showers in the calorimeter [1], neither of the charged tracks in the inner detector. In addition, this fast simulation package smears cluster and jets rather than their constituent cells[2]. So in Atlfast, the detector-dependent parameters are tuned to what is expected for the performance of the ATLAS detector from full simulation and reconstruction.

There is only a parameterization of the hadronic calorimeter energy resolution, as well as a reasonably accurate one for photon, electrons and muon energy or momentum resolution. A simulation of the efficiency in the Inner detector and the reconstruction of the helix track parameters are also provided with separate parameterizations on the resolutions for muon, electron and pion tracks.

The parameterizations used in Atlfast were derived from full simulation studies:

- **Resolution in EM Calorimeter** (photons and electrons candidates are smeared with this parameterization), for barrel ($|\eta| < 1.4$) and for endcaps ($|\eta| > 1.4$) regions, respectively:

$$\frac{\sigma(P_T)}{P_T} = \frac{0.245}{p_T} \oplus 0.007 \tag{4}$$

$$\frac{\sigma(P_T)}{P_T} = \frac{0.306 * ((2.4 - \eta) + 0.228)}{p_T} \oplus 0.007 \tag{5}$$

- **Resolution in the HAD Calorimeter** (hadrons are smeared with this parameterization) for central barrel ($|\eta| < 3$) and for extender barrel ($|\eta| > 3$) regions, respectively:

$$\frac{\sigma(E)}{E} = \frac{0.5}{\sqrt{E}} \oplus 0.03 \tag{6}$$

$$\frac{\sigma(E)}{E} = \frac{1.0}{\sqrt{E}} \oplus 0.07 \tag{7}$$

- **Resolution in the Inner Detector** (parameterizations for muon, electron and pion tracks), in the simplest case:

$$\frac{\sigma(P_T)}{P_T} = 0.00036 p_T \oplus 0.013 \tag{8}$$

[1] Excepting the FastShower package done by K. Mahboubi et al. (Mainz) which can be used in Atlfast to give transverse shower shape parameterization at a granularity of 0.1 x 0.1

[2] Electromagnetic and hadronic cells in Atlfast have the same granularity $\Delta\eta$x$\Delta\phi$ = 0.1 x 0.1, while in the real ATLAS detector EM cells have lower size $\Delta\eta$x$\Delta\phi$ ~0.0025 x 0.025

and in the case where the track resolution depends on η values:

$$\frac{\sigma(P_T)}{P_T} = 0.0005(1 + |\eta|^{\frac{10}{7000}})p_T \oplus 0.012 \quad (9)$$

Only when the high luminosity option is selected, pile-up events are included in the parameterization in a simple mode as a deterioration of the energy resolution. Anyway, this analysis will be done at low luminosity, so pile-up events are not included.

So, some physical aspects like the overlap can be studied by Atlfast, however when the influence of the behaviour of the hadronic shower is bigger it is needed to continue the analysis with Full Simulation[15] where the detector response is modelled in a very accurate way, making use of the GEANT package[16].

4 Generation with PYTHIA 6.2

For this analysis we have generated 1000 events of QCD jets, applying the following conditions in Pythia[17] program:

- generation of jets with different range of transverse momentum: 20-40 GeV, 40-80 GeV, 80-160 GeV, 160-320 GeV, 320-640 GeV and 640-1280 GeV, to provide adequate statistics in the full range of E_T [3], showing the variation of the improvement in the resolution with the energy.
- In a first step, the studies have been done without including neither Underlying Events nor Minimum bias effects. In section 8th of this note, the effect of the additional low p_T particles that they induce is investigated and their contribution to the deterioration of the resolution.
- ISR and FSR, initial and final state radiation, are included in the analysis because they influence in the final direction of the jet.
- η_{parton} <5.0, i.e., partons come from hard scattering are generated only inside the calorimeter coverage.

5 Reconstruction and Simulation with Atlfast

For the reconstruction of the jets of quarks and gluons we have used in this work the Release 6.2.0 of the ATHENA-Atlfast package, and the following conditions have been selected in the AtlfastStandarOptions file:

- jets are reconstructed using the Cone algorithm for two different values of the radius DR: 0.4 and 0.7, where DR=$\sqrt{\Delta\eta^2 + \Delta\phi^2}$. We will see how the improvement in the resolution changes with the radius.

[3]The separation between the values is bigger and bigger because the probability to have jets is smaller and smaller, due to the shape of the distribution of the p_T of the jets.

- A minimum value of the P_T of the jet is required in order to prevent excessive merging of noise and energy not associated with hard scattering. We take different P_T^{min} values depending on the radius of the cone: for R=0.4, P_T^{min}= 15 GeV is taken, while for R=0.7, P_T^{min}= 20 GeV is taken. These values for the P_T^{min} are chosen such that the number of jets has decreased and stabilized.

- Finally, jets are generated only into the inner detector coverage ($|\eta_{jet}| < 2.5$) because later we are using in combined way calorimeter and tracking information. We apply $|\eta_{jet}|$ <2.0 in order to assure the completed reconstruction of the jet from the cone with R=0.4 and 0.7.

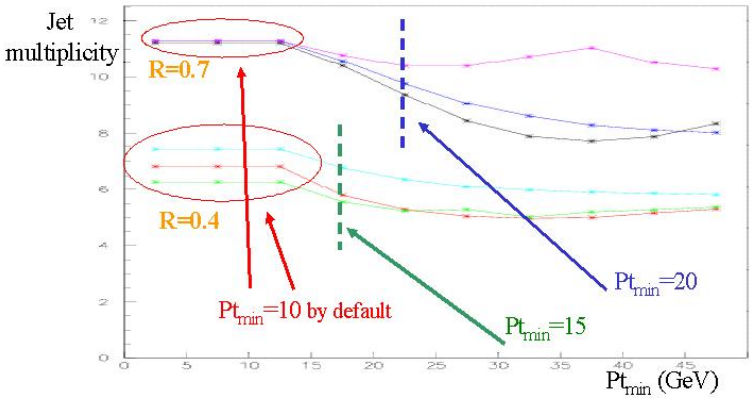

Figure 2: Multiplicity of jets for the two radius of the jet cone: R=0.4 and 0.7, and for the E_T jet ranges of 20-40 GeV, 40-80 GeV and 80-160 GeV. The best P_T^{min} cut for R=0.4 is ∼15 GeV and for R=0.7 is 20 GeV, values for which the number of jets has decreased and stabilized.

In the following table appear the numbers of generated QCD jets for the different cases after applying all these selection criteria.

	Number of QCD jets in Atlfast:					
	20-40	40-80	80-160	160-320	320-640	640-1280
R =0.4	649	1628	2276	2993	3666	4282
R =0.7	288	1414	2091	2755	3369	4009

6 Particle level composition of the jets

We reconstructed the jet energy deposited in the calorimeter summing the energy of the particles that fall inside the cone of R=0.4 or 0.7 centred at η_{jet}-ϕ_{jet} coordinates. Only stables particles are considered. These particles are mainly: a few tens of charged hadrons ($\pi^{\pm}$ and $k^{\pm}$), a similar amount of photons (coming from π^0 decay into $\gamma\gamma$), a lesser extent neutral hadrons(k_{lo} and neutrons) and very few leptons ($e^{\pm}$, $\mu^{\pm}$ and neutrinos).

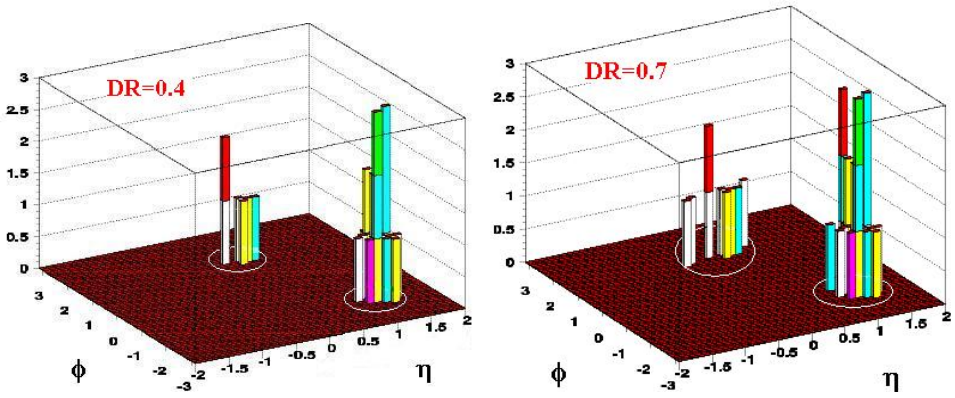

Figure 3: Reconstruction of the jet from stable particles inside a cone of radios 0.4 and 0.7 after passing a certain selection.

Moreover, we apply the following selection criteria, before obtaining the final results and plots:

- a minimum value of the transverse energy of the charged particles, E_T >0.5 GeV , in order to remove the particles with very small value transverse energy which do not reach the calorimeters and loop inside the inner detector cavity.
- only selected particles deposited in the calorimeter into the eta values of the inner detector coverage ($|\eta_{jet}| < 2.5$) due to the combined used of calorimeter and tracking measurements.

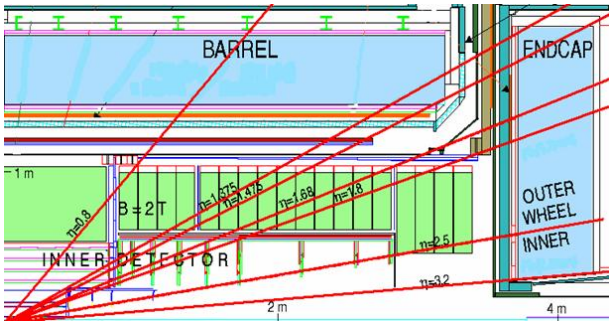

Figure 4: View of the ATLAS Inner detector and Calorimeters system. The coverage in of the Inner Detector is $|\eta| < 2.5$.

6.1 Number of particles forming the jets

The next table shows the number of selected stable particles for various cases of E_T range. Some initial observation can be made:

- there are mainly charged hadrons and photons
- the amount of leptons ($e^{\pm}$, $\mu^{\pm}$ and neutrino s) has been negligible (below 0.5%).
- the multiplicity of the charged and neutral particles is similar

R=0.4	Total Partc	Charged Had		Neutral Had		Photons	
	in jet	per jet	%	per jet	%	per jet	%
40-80 GeV	13.2	6.17	**46.6**	0.94	7.1	6.02	45.5
80-120 GeV	17.2	8.17	**47.1**	1.11	6.4	7.92	45.7
160-320 GeV	20.9	9.97	**47.3**	1.30	6.1	9.63	45.7

R=0.7	Total Partc	Charged Had		Neutral Had		Photons	
	in jet	per jet	%	per jet	%	per jet	%
40-80 GeV	13.4	6.39	**47.6**	0.95	7.0	6.02	45.0
80-120 GeV	17.6	8.43	**47.1**	1.13	6.3	8.17	47.5
160-320 GeV	21.7	10.32	**47.3**	1.34	6.1	9.98	45.9

Table 1: Number of selected stable particles into jets for various ranges of E_T for R=0.4 and 0.7.

If we compare the results for different values of E_T range of the same radius:

- The number of particle per jet increase with the transverse energy[4]
- Similar contribution from charged hadrons ($\pi^{\pm}$ and $k^{\pm}$) and photons ($\pi^0 \rightarrow \gamma\gamma$)

Also if the numbers of particles from the different values of the radius of the reconstructed jet cone are compared we can obtain some conclusion:

- The general trend is the same for R=0.4 and R=0.7
- The number of particles per jet in the R=0.7 case is about 0.5 to 1 particle more than in the case of R=0.4.

6.2 Jet E_T deposited in the calorimeter

The E_T deposited by selected stable particles has been analysed, and values of the total E_T of jets reconstructed from MC Truth particles and by Atlfast are similar, as you can see for the case of jets with 40-80 GeV and DR = 0.4. It means the reconstruction of the jets from the selection of the stable particles in the cone has been well done.

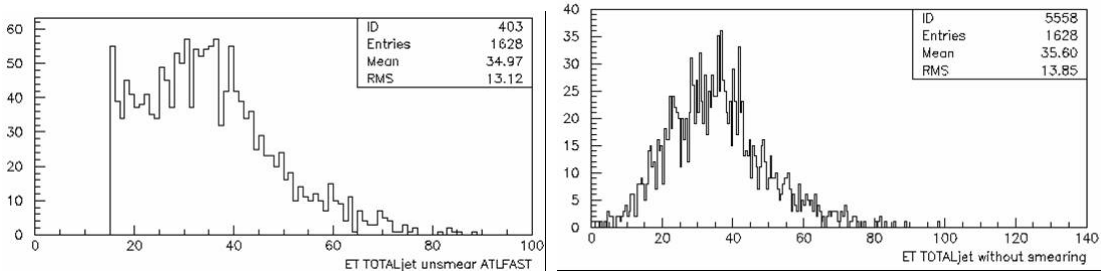

Figure 5: E_T total of reco jets from particles and from Atlfast for R=0.4 and Pt jet 40-80 GeV.

[4]Two effects may play a role. As the energy of the parton increases more particle are generated during the fragmentation. At the same time, they get more collimated.

Similarly, in the following tables the different values of E_T deposited by the stable particles are shown for various cases of E_T range. We observe that:

- The contribution of the E_T deposited by charged hadrons is the longest, about 2/3 parts of the total.
- The leptonic contribution ($e^{\pm}$, $\mu^{\pm}$ and neutrons) is negligible (below 1%).

R=0.4	Charged Had		Neutral Had		Photons	
	per jet	%	per jet	%	per jet	%
40-80 GeV	22.6	**61.2**	4.6	12.5	9.2	25.2
80-120 GeV	40.4	**61.3**	7.8	11.8	16.9	25.6
160-320 GeV	69.1	**61.4**	13.1	11.9	28.9	25.7

R=0.7	Charged Had		Neutral Had		Photons	
	per jet	%	per jet	%	per jet	%
40-80 GeV	24.2	**61.1**	4.9	12.4	9.9	25.2
80-120 GeV	42.6	**61.3**	8.2	11.8	17.8	25.7
160-320 GeV	73.5	**61.4**	14.0	11.7	30.8	25.7

Table 2: E_T of selected stable particles into jets for various ranges of E_T for R=0.4 and 0.7.

Again, if we compare the results of transverse energy deposited by the particles inside the cone for different E_T ranges with the same R, we can draw several conclusions:

- The E_T deposited by particles increase as the E_T range of jet is bigger.
- The contribution from charged hadrons is more than twice that from photons, as expected since the gammas come from π^0 decay.
- Same proportion in % of each type of particle respect the total of particles (it must be independent of R, it only depends on physics).

Finally, comparing the E_T deposited by particles for the two radiuses DR of the reconstructed jet cone:

- The results for R=0.7 are similar than for R=0.4, in the two cases E_T particles increase as the E_T jet is bigger.
- The E_T deposited for the particle per jet is bigger in R=0.7 than in R=0.4, as R increase the proportion of the initial parton energy inside the cone is bigger.
- The energy sharing between particles does not change for the two cone radii.

6.3 Jet E_T fraction carried by charged hadrons

In view of the previous tables and numbers, we can extract two important results about charged hadrons:

- Their number is $\sim 47\%$ of the total of particles.
- Their transverse energy deposited is $\sim 60\%$ of the total of energy.

7 Study of the overlap of particles

We are going to apply the Energy Flow Algorithm to the charged hadrons, but not to all, only to the charged hadrons hitting calorimeter cells without overlap with neutral particles. So, we need:

- To define the calorimeter cell hit by the particles
- To do a classification of the cell based on the type of particles hitting it.

A grid of 81 "cells" around the central coordinate η_{jet}-ϕ_{jet} of the reconstructed jet is defined. These "cells" correspond to the energy projected in the tower with a granularity $\Delta\eta$ x $\Delta\phi = 0.1$ x 0.1, as in the Atlfast's code. We want to analyse:

- the type of particle which hit in each "cell" (charged or neutral particle): in order to do a classification of the "cells".
- the number of particles inside each classified "cell".
- the transverse energy deposited in each "cell".

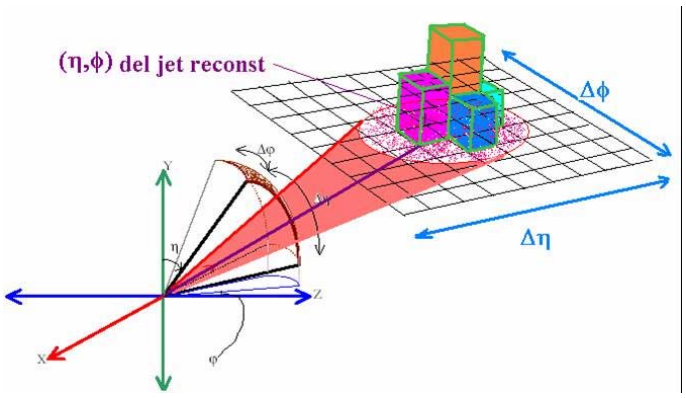

Figure 6: A grid of "cells" with a granularity $\Delta\eta$ x $\Delta\phi = 0.1$ x 0.1 is defined around the central coordinate η_{jet}-ϕ_{jet} of the reconstructed jet.

7.1 Classification of the "cells"

In order to apply later the Energy Flow Algorithm, "cells" will be divided into three classes, and for each class a different method to determine the energy collected in the "cell" is adopted, which relies on the kind of particles hitting the cell.

- **Charged cells:** "Cells" hit only by charged hadrons ($\pi^{\pm}$ and $k^{\pm}$).
- **Neutral cells:** "Cells" hit only by photons.
- **Mixed cells:** "Cells" hit by a mixture of charged and neutral particles.

In the last class of "cells" the overlap between charged hadrons and photons or neutral hadrons will be analysed.

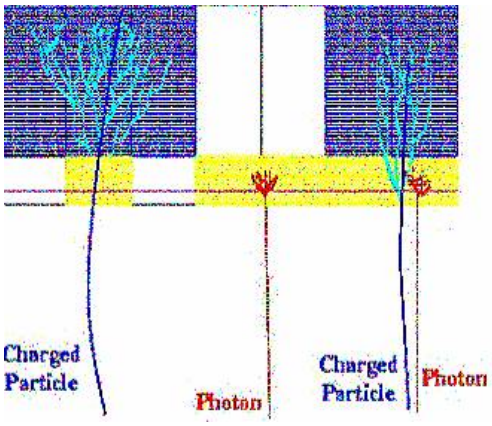

Figure 7: The classification of cells depends on which particle fell in it. Only charged hadrons: Charged, only photons: Neutral and a mixing between neutral and charged particles: Mixed Cells.

Figure 7 shows the frequency at which "cells" are classified as charged, neutral and mixed. The density is higher in the center. Overlap takes place mostly in the center or in the first "ring" (see also Figure 8).

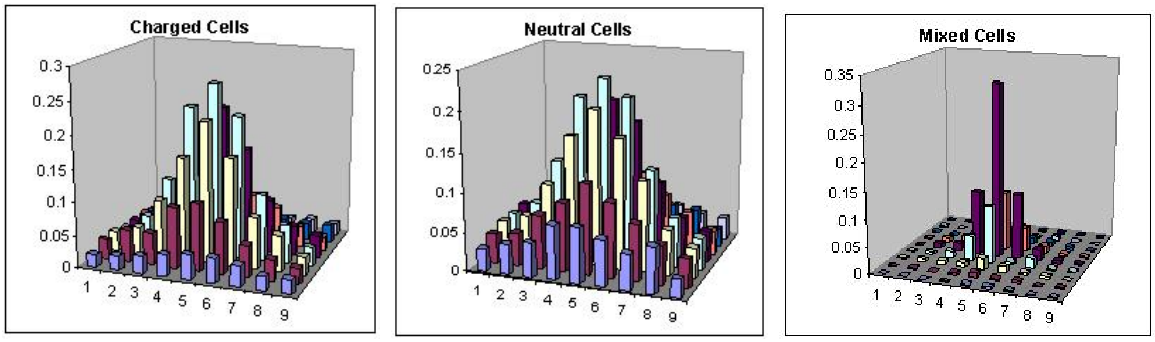

Figure 8: Number of times that each "cell" is classified as Charged, Neutral or Mixed Cell per jet in the plane η-ϕ, in the case of 40-80 GeV with DR=0.4. Most are in the central region of the cone (1 means DR$\leq$0.1).

In Figure 8, the number of the classified "cells" in analysed as a function of the radius DR. The most of particles are in the central "ring"($DR < 0.1$), overall in the case of the Mixed Cells, which implies that the overlap will be an important effect.

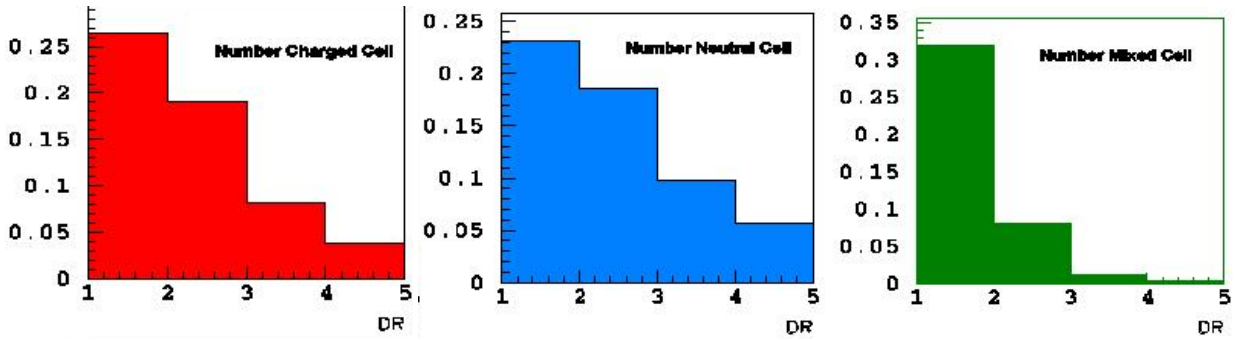

Figure 9: Number of times that each "cell" is classified as Charged, Neutral or Mixed Cell per jet as a function of the radius DR, in the case of 40-80 GeV with DR=0.4. Most are in the central "ring".

The next table shows the cell classification for the total grid in the η-ϕ plane (DR<0.4) and for the central region (DR<0.1), where most of the E_T is deposited.

R=0.4	Charged cells (%)		Neutral cells (%)		Mixed cells (%)	
	DR<0.4	DR<0.1	DR<0.4	DR<0.1	DR<0.4	DR<0.1
40-80 GeV	40.1	**18.6**	48.8	**18.6**	11.1	**8.7**
80-160 GeV	38.5	**16.5**	45.7	**16.5**	15.8	**12.0**
160-320 GeV	36.4	**14.8**	44.6	**14.8**	19.0	**13.9**

Table 3: Proportion of Number of classified cells for the total grid (DR<0.4) and for the central region (DR<0.1).

Also the E_T deposited in Charged Cells by the charged hadrons, in Neutral Cells by the photons and in Mixed Cells by the mixing of neutral and charged particles for each one of the 81 "cells", has been evaluated. The next plots show the results for jet range at 40-80 GeV.

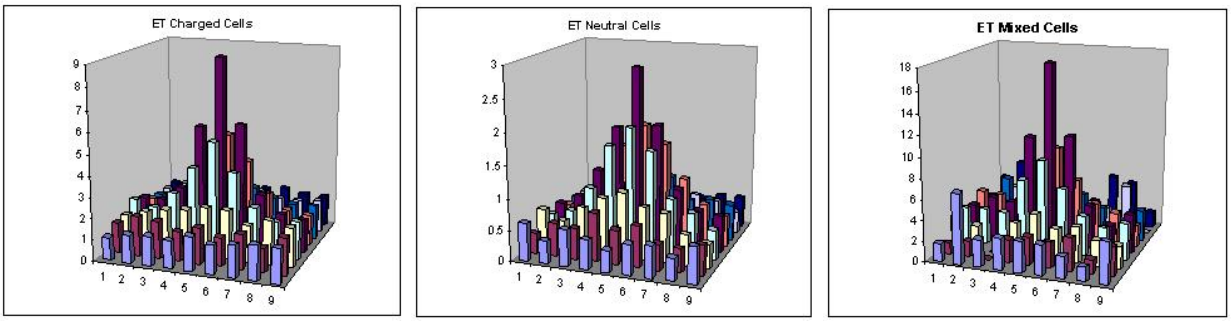

Figure 10: E_T deposited in the η-ϕ plane by charged hadrons in Charged Cells, photons in Neutral Cell and mixing neutral-charged particles in Mixed Cells per jet at 40-80 GeV with DR=0.4.

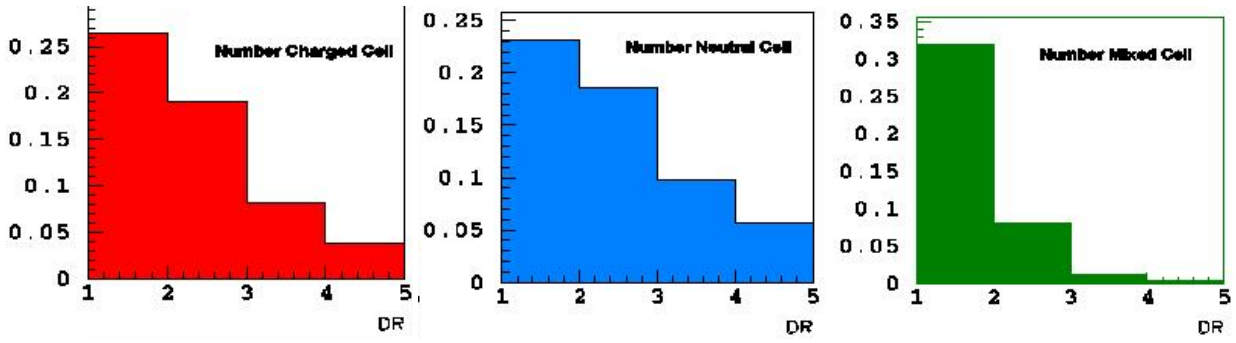

Figure 11: E_T deposited in Charged, Neutral and Mixed "cells", as a function of the radius DR, in the case of 40-80 GeV with DR=0.4.

Finally, next table shows the mean value of the E_T deposited in each jet and the proportion in % respect to the total E_T of the reconstructed jet from the stable particles. Again, the values are shown for some range of E_T of the jet for the case of DR=0.4

R=0.4	ET jet	Charged cells		Neutral cells		Mixed cells	
	(GeV)	per jet(GeV)	(%)	per jet(GeV)	(%)	per jet(GeV)	(%)
40-80	35.50	16.31	**45.81**	6.73	18.90	12.56	35.28
80-160	65.94	21.84	**33.78**	8.67	13.41	35.28	54.58
160-320	94.20	23.72	**25.18**	9.59	10.19	60.68	64.41

Table 4: E_T deposited in the whole of classified cells respect to the total E_T of the reconstructed jet from the stable particles..

This table shows that up to $\sim 45\%$ on the total E_T, in the best case, comes from charged hadrons. So the Energy Flow algorithm will be applied to an important portion of the jet energy. However this proportion of energy decreases quickly as the range of E_T of the jets get larger. At the same time, the energy deposited in the Mixed Cell increases, because the overlap of particles is bigger. So, the gain of resolution with the application of the algorithm will decrease with energy.

7.2 Jet E_T resolution with and without Energy Flow

The energy resolution of the photons into Neutral cells is calculated according to the parameterization of the EM Calorimeter. The energy resolution of the particles into Mixed Cells is approximated [5] by the parameterization of the Hadronic Calorimeter.

[5]This is an approximation because in Mixed Cells, as well as hadrons, there are also electrons and photons and the resolution of their energy is calculated for simplicity from the parameterization of the Hadronic Calorimeter instead of by the EM Calorimeter

For the energy deposited by the charged hadrons into the Charged cells, usually the HAD calorimeter parameterization is taken by Atlfast, but since we apply Energy Flow method, we are going to substitute the energy calorimeter resolution by the track momentum resolution of the inner detector.

You can see in the next plots for the case of 40-80 GeV and DR=0.4, the difference between the energy resolution of the charged hadrons from HAD Calorimeter, $\sim 13\%$, and the momentum resolution of the track from Inner Detector,$\sim 1\%$, much better.

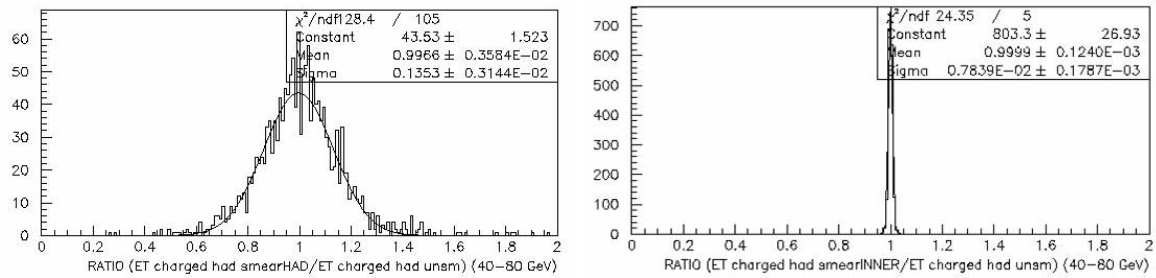

Figure 12: The energy resolution of the charged hadrons from HAD Calorimeter, $\sim 13\%$, and the momentum resolution of the track from Inner Detector,$\sim 1\%$,for the case of 40-80 GeV and DR=0.4.

This improvement in the resolution of the charged hadrons energy imply a improvement in the total deposited E_T resolution $\sim$40% for 40-80 GeV and DR=0.4, as the next distribution show, since applying Had Calorimeter parameterization the resolution is $\sim$7.9% while if the parameterization of the inner detector is applied it reduces to $\sim$4.8%.

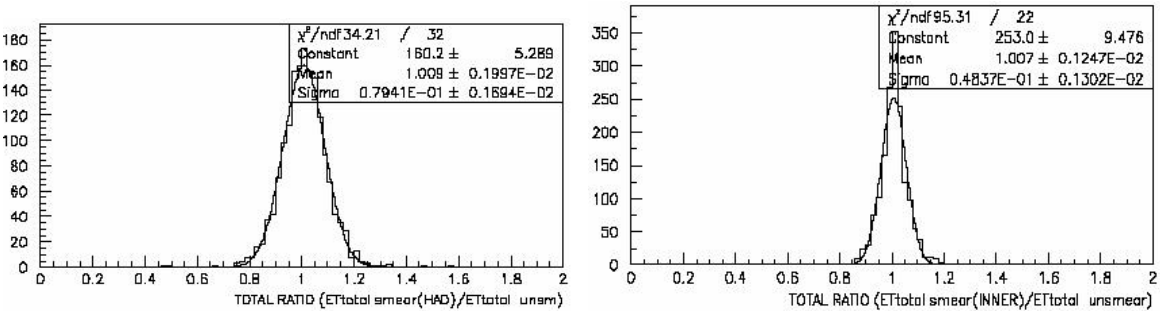

Figure 13: For the range of 40-80 GeV and DR=0.4, the resolution in the E_T of the jet applying Had Calorimeter parameterization is $\sim$7.9% while if the parameterization of the inner detector is applied the resolution improves ($\sim$4.8%).

The following tables show the jet energy resolution for the two scenarios (hadronic calorimeter energy resolution and track momentum resolution from inner detector) and the relative improvement [6].

R=0.4	RMS (HAD)	RMS (INNER)	Improvem(%)
20-40 GeV	0.094	0.046	51.5
40-80 GeV	0.079	0.048	**39.0**
80-160 GeV	0.062	0.042	**31.0**
160-320 GeV	0.051	0.039	**23.6**
320-640 GeV	0.041	0.034	**16.9**
640-1280 GeV	0.032	0.029	**9.6**

R=0.7	RMS (HAD)	RMS (INNER)	Improvem(%)
20-40 GeV	0.091	0.032	64.7
40-80 GeV	0.076	0.049	**35.7**
80-160 GeV	0.062	0.043	**30.7**
160-320 GeV	0.049	0.039	**20.4**
320-640 GeV	0.039	0.033	**16.6**
640-1280 GeV	0.031	0.028	**9.5**

Table 5: Jet energy resolution for the two scenarios (hadronic calorimeter energy resolution and track momentum resolution from inner detector) and the relative improvement. The range of 20-40 GeV has been discarded because there is a bias in the jet selection.

With this simplified model, we see that there is potentially an important gain in resolution. From the results, we can extract that the improvement decreases as the jet energy increase.

[6] The range of 20-40 GeV has been discarded because there is a bias in the jet selection, due to the cuts applied in the generation of the jets are close to the jet energy.
To generate jets in Atlfast, we applied cuts in the minimum value of the P_T of the jets:
- P_T^{min}= 15 GeV for DR=0.4 and P_T^{min}= 20 GeV for DR=0.7.

In the 20-40 GeV range the mean value of E_T for the reconstructed jets from the selected stables particles are very close to this cut:
- E_T Mean = 21.65 GeV for DR=0.4 and E_T Mean = 24.38 GeV for DR=0.7.

So, there may be an important portion of the candidate jets that are not considered in the analysis.

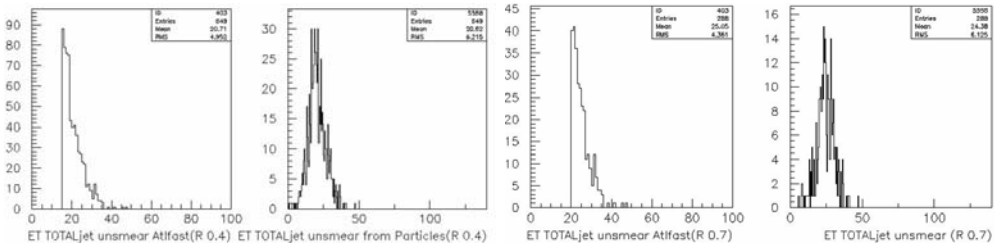

This improvement in the resolution is larger at low P_T, reaching values up to ∼40%. At a few 100 GeV the overlap between charged and neutral particles increases and the gain in resolution of the energy jets becomes marginal.

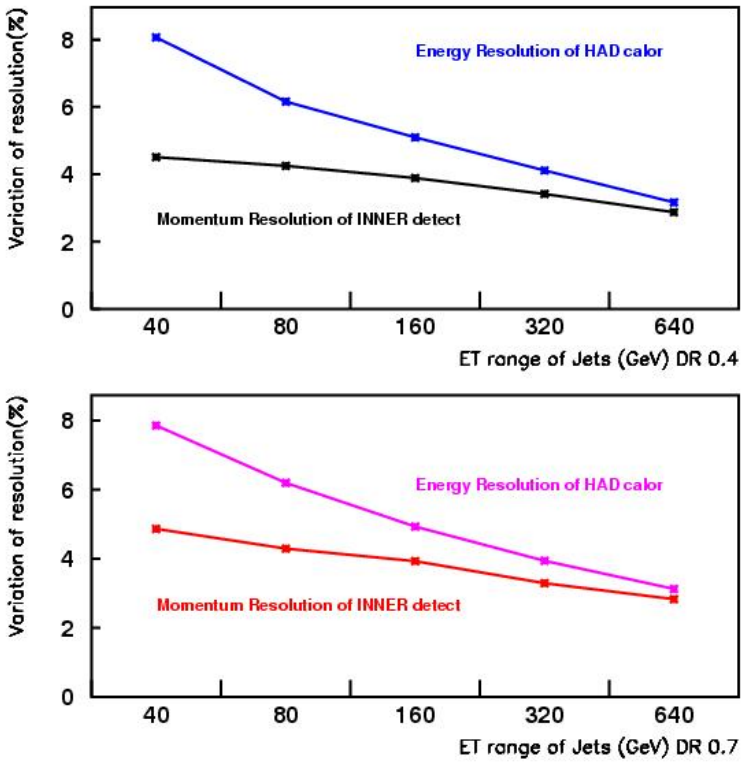

However, the figure quoted should not be interpreted as a realistic estimate of performance because showers fluctuation have not been included and will limit the improvement.

8 P_T spectrum of particle, Underlying Events and Minimum Bias

As we have seen the best results of the Energy Flow Algorithm have been obtained at low E_T. In this section, we are going to study the range of 40-80 GeV and the cone DR=0.4 in more details.

8.1 Transverse Energy of single particles

To continue the Energy Flow analysis in Full Reconstruction, we need to calculate the transverse energy deposited by the particles which form the jets (mainly pions and photons). In Figure 13, the E_T distributions of pions and photon are shown for low E_T jets. The average E_T is around ∼2 GeV for pions and ∼1 GeV for photons, about

half the value of hadrons as expected, taking into account the cut off at 0.5 GeV for charged particles.

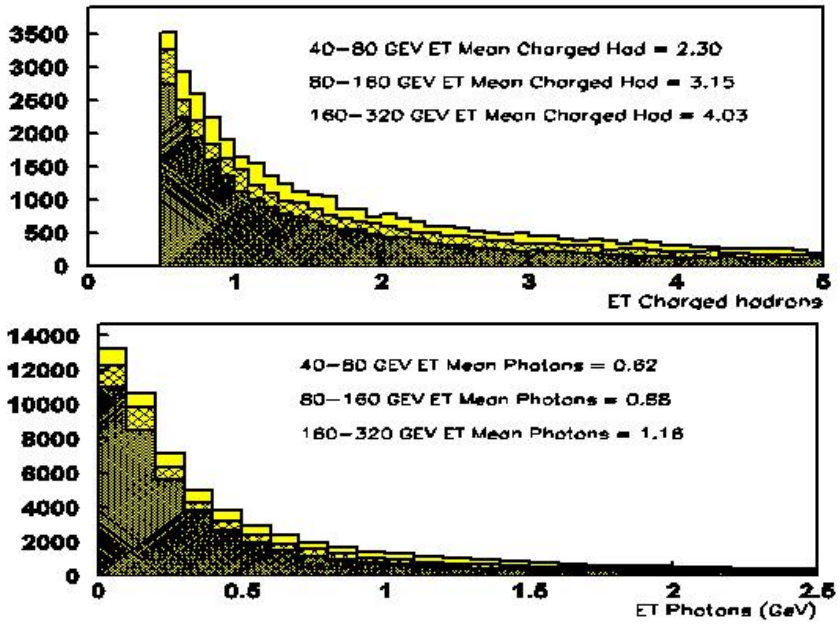

Figure 14: The average E_T distributions of pions and photons for low E_T jets with cone DR=0.4.

Therefore, the fraction of low P_T particle inside the jet cone of radius 0.4 is around the 25% for charged particles and ∼18% for neutral particles, the rest of the jet is composed by particle of high P_T, so the bulk of the jet energy is carried by a small number of the most energetic particles. Taking into account this information, we must no work only with set of particles of low P_T when we want to compare Monte Carlo simulation results with real data.

On the other hand, we must consider for future analysis in Full Simulation the problem that the Energy Flow method can generate for jets with energetic charged fragments. Compared to soft charged fragments, the effect of the magnetic field on these particles is small and, therefore, they enter the calorimeter in the same region where also the photons (from the π_0 decay) deposit most of their energy, and the probability of the overlap between charged and neutral particles inside the calorimeter cell will be increased.

8.2 Effect of Underlying Events

The general analysis shown in this note has been done without considering neither Underlying Events nor Minimum Bias Events, only taking into account the 'Hard scattering' components, that consists of the out coming two jets which come from a hard 2-to-2 parton scattering which interact at short distance with large P_T transferred.

Protons are not fundamental particles. They are formed by quarks and gluons. In addition to the hard scattering, multiple interactions can take place: a second, a third... softer2-to-2 scattering, and they contribute to the 'Underlying Events'.

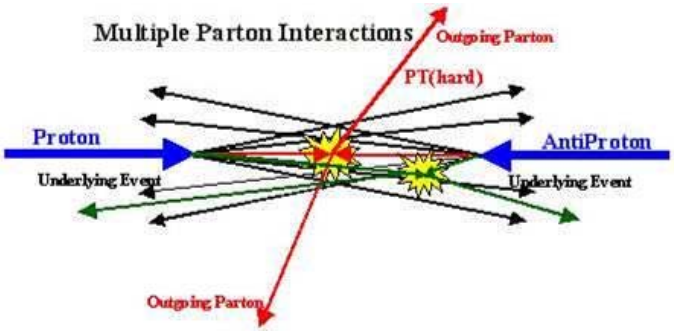

Figure 15: QCD Monte-Carlo models simulation of $p - \bar{p}$ collision in which a hard 2-to-2 parton scattering with PT(hard) has occurred. The resulting event contains particles that originate form the 2 ingoing partons (plus ISR and FSR) and particles that come from the break-up of the $p - \bar{p}$ (beam-beam remnants). Underlying Events is everything except the 2 outgoing hard scattered jets.

So, the UE Corrections consider all the contributions to the jet energy not coming from the original partons, i.e., is everything except the hard scattering and consist of:

- **the beam-beam remnants** in each incoming beam particle behind the hard scattering.
- **Multiple interactions:** a second, a third... softer 2-to-2 parton scattering in addition to the hard scattering.
- **ISR and FSR:** Emission and interaction between gluons and quark out of the hard scattering.

In our analysis, we have generated the QCDjets including the effect of ISR and FSR because they have influence in the final direction of the jets as well as the multiplicity of them. So, when we compare here QCDjets with Underlying Events we try to understand mainly the effect to add multiple interactions in the analysis.

Due to UE, the jets measured may be significantly more energetic than the jets intended by nature, so if we include the UE in the analysis we expect to find an increase of the transverse energy associated with each reconstructed jets

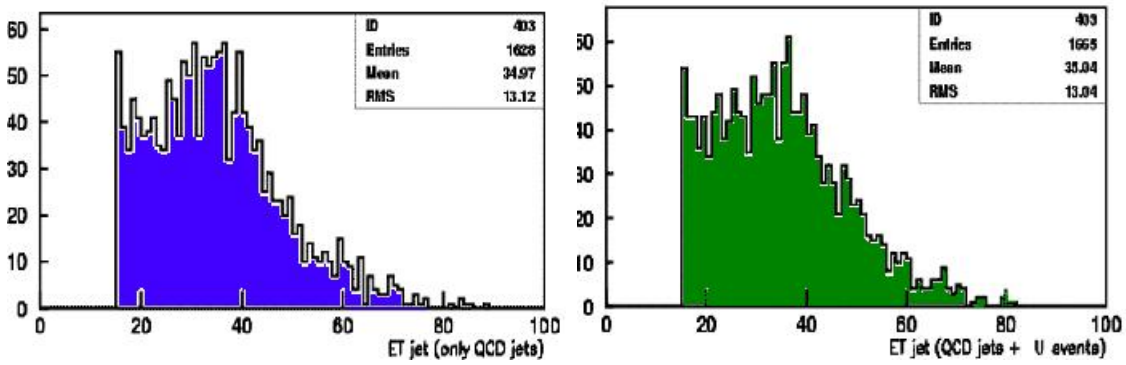

Figure 16: The E_T of the reconstructed jet increased from a mean of 34.97 GeV to a mean value of 35.04 GeV when the Underlying Events are included.

On the other hand, Underlying Events has also an influence in the multiplicity of the particles which form our reconstructed jets and we expect to find an increase in the multiplicity of charged hadrons and photons, as it can be seen in the next distributions.

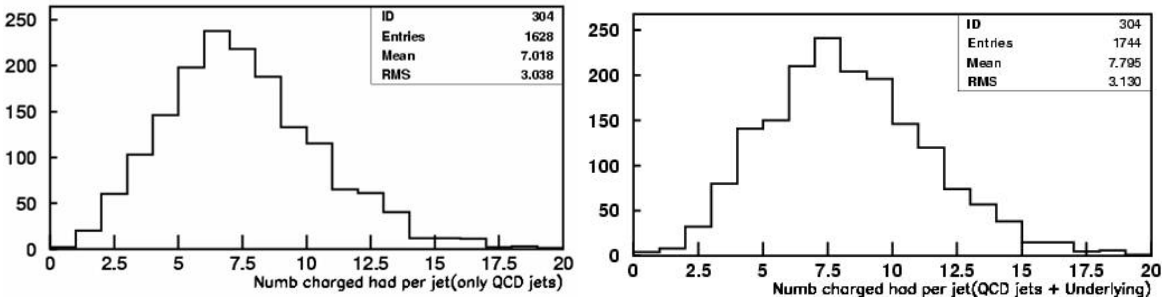

Figure 17: The multiplicity of charged hadrons increase from ∼7.0 charged hadrons per jet to ∼7.7, i.e., around 10%, when the Underlying Events are included.

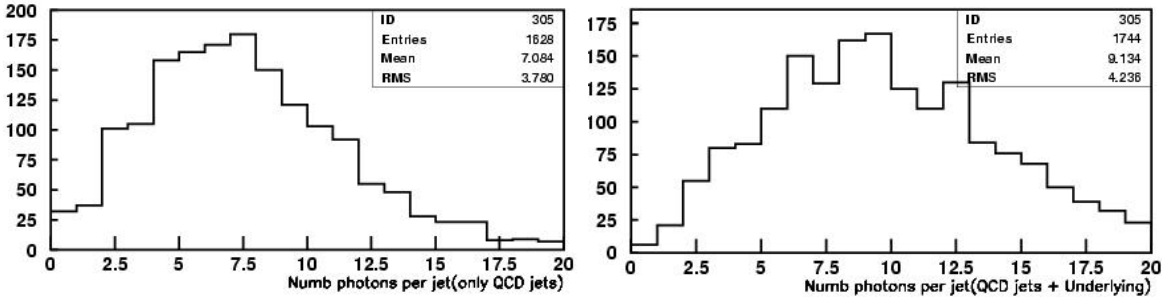

Figure 18: The multiplicity of photons increase from ∼7.1 photons per jet to ∼8.1, i.e., around 14%, when the Underlying Events are included.

8.2.1 Occupancy of cells and Density particles per event in unit of rapidity

We compare the number of particles per event that hit in each calorimeter cell with a granularity of 0.1x0.1 in the $\eta - \phi$ plane in the case to have generate only QCDjets (with ISR and FSR included) to the case where the multiple interaction is switched on and there are Underlying Events. Therefore we analysed the density of particles per unit of pseudorapidity in order to compare with previous analysis of MB events.

	Occupancy of Cell (partc/cell)		
	Total Particles	Total Partic ($P_T$cut)	Charged Had ($P_T$cut)
UE+jets	0.085	0.060	0.017
Underlying Events	0.055	0.036	0.009
QCDjets	0.030	0.024	0.008

	Density Particles in eta (partc/eta)		
	Total Particles	Total Partic ($P_T$cut)	Charged Had ($P_T$cut)
UE+jets	54	38	11
Underlying Events	35	23	6
QCDjets	19	15	5

Table 6: Occupancy of cell (partc/cell) with a granularity of 0.1x0.1 in the $\eta - \phi$ plane and density particles in eta (partc/eta) for only QCDjets and for Underlying events + QCDjets.

The mean value of the particle density, dN/dη, decreases when we applied the P_T cut to the charged particles (P_T>0.5 GeV).

These numbers have been extracted from the "total particles versus eta" distributions with a bin equal to the granularity of the calorimeter (i.e. $\Delta\eta$ =0.1). Also the histograms have been normalized by 64 because we have supposed that there is symmetry in ϕ coordinate.

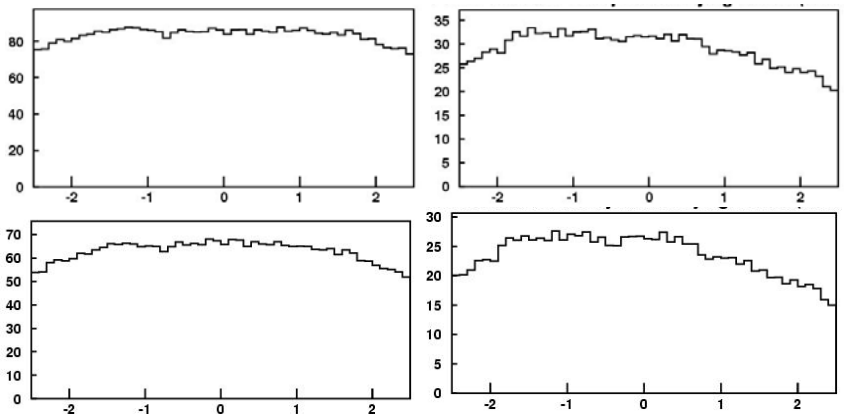

Figure 19: Number of total particles which hit each cell of granularity of 0.1x0.1 for QCDjets with underlying event (left-side) and without it (right-side) in 1000 events. On the top, distributions without applied P_T cut for charged particles and on the bottom with the cut off.

8.3 Effect of Minimum Bias Events

Minimum Bias studies are important in order to understand the background to signal events. For this reason Minimum Bias studies are used to predict radiation damage to the detector created by the scattered protons.

The cross section for hadron-hadron collision consists of four major processes these being non diffractive, single diffractive, double diffractive and elastic. The processes of interest for tracking studies are the inelastic non-diffractive with a cross section of the order of ∼70 mb from TDR studies (Pythia 5.7). More recently, the best fit to experimental data with Pythia 6.2 predict a cross section of 55mb.

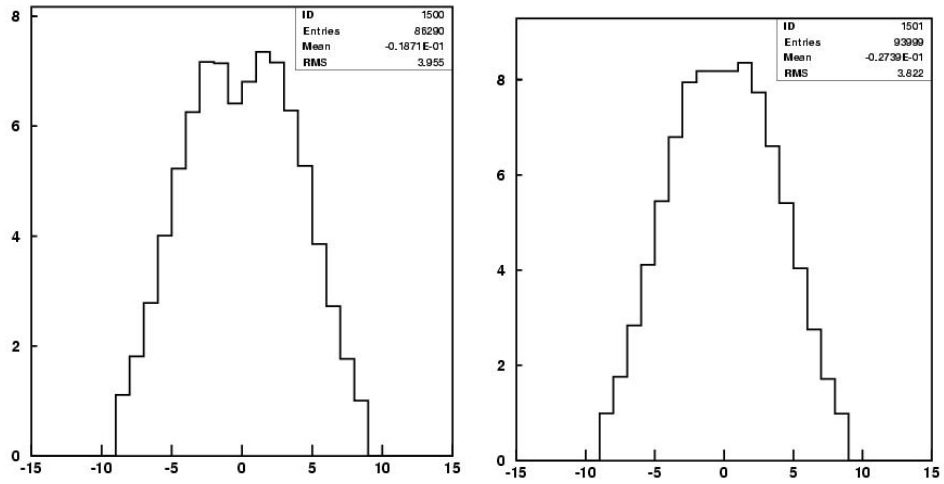

Figure 20: Density of charged and neutral particles in the simulated Minimum Bias events for unit of rapidity

The non-diffractive inelastic events, used to simulate Minimum Bias Production, were generated using Pythia 6.203. In the previous plot it is possible to see the mean multiplicity of charged and neutral particles in the simulated Minimum Bias events. In the region $|\eta| < 5$, the average number of charged particles (no pt cut applied) is 7 per MB events and per unit of rapidity, while for neutral particles it is 8.5. These are similar results to which appear in the Calorimeter Performance and TDR studies. The differences are due to the multiplicity of the particles depends on the model used for the parton-parton interactions in the generators, as is shown in the A. Moraes studies[19].

8.3.1 Pile-Up Events at low luminosity

At high luminosities, multiple collisions within one beam-crossing will be inevitable, causing signal events to have several Minimum Bias events superimposed. The pile-up of these events on top of single particles is essential for realistic studies.

In each bunch crossing, the number of Minimum Bias events produced is described by a Poisson distribution with a mean determined by the Minimum Bias cross section and the operating luminosity of the LHC. The expected average number of MB events

per bunch crossing is expected to be 23 for high luminosity ($10^{34} cm^{-2} s^{-1}$) running while for low luminosity ($10^{33} cm^{-2} s^{-1}$), an average of 2.3 minimum bias events per bunch crossing are expected.

We have generated Pile-Up events at low luminosity (i.e., leading a Poisson distribution with a mean value of 2.3 events of Minimum Bias per bunch crossing). Pythia generator contains an option to generate several events and put them one after the other in the event record. The program needs to know the assumed luminosity per bunch crossing expressed in mb^{-1}, for the LHC case these values are:

- 0.250 for high luminosity ($10^{34} cm^{-2} s^{-1}$)

- 0.025 for low luminosity ($10^{33} cm^{-2} s^{-1}$)

Multiplied by the cross section for the Pile-Up processes studied, this gives the average number of collision per beam crossing. Pythia take the Pile-Up events to be of the Minimum Bias type (with diffractive or elastic included or not). In our case have taken into account only the non-diffractive inelastic low P_T events.

8.3.2 Occupancy of cells and Density particles per event in unit of rapidity

Again we compare the number of particles per event that hit each calorimeter cell of 0.1x0.1 in the $\eta - \phi$ plane with and without the additional Pile-Up events.

	Occupancy of Cell (partc/cell)		
	Total Particles	Total Partic cut ET	Charged Had cut ET
MB Events	0.024	0.016	0.0035
Pile-Up	0.045	0.031	0.0075
QCDjets	0.030	0.024	0.0080

	Density Particles in eta (partc/eta)		
	Total Particles	Total Partic cut ET	Charged Had cut ET
MB Events	15	10	2.2
Pile-Up	29	20	4.8
QCDjets	19	15	5

Table 7: Occupancy of cell (partc/cell) with a granularity of 0.1x0.1 in the $\eta - \phi$ plane and density particles in eta (partc/eta) for QCDjets, Minimum Bias events and Pile-Up events at low luminosity.

In this case, when we applied the P_T cut to the charged particles (P_T>0.5 GeV) to the MB and Pile-Up events, the value dN/dη falling a lot because it is characterised by low P_T values. So the effect of Pile-Up events in the signal with low P_T is very small.

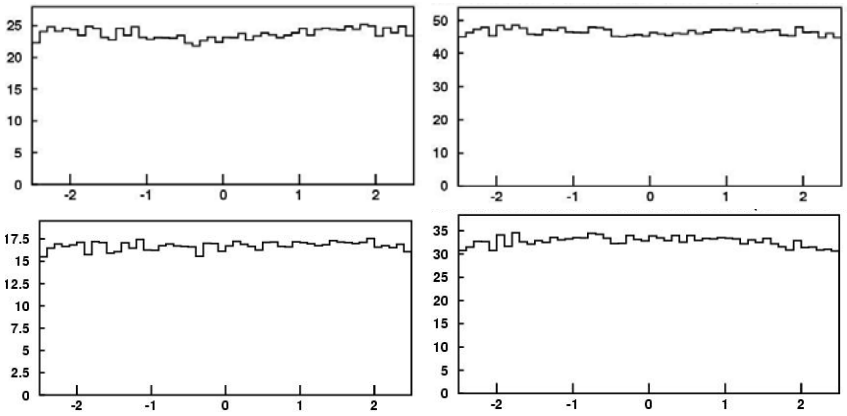

Figure 21: Number of total particles which hit each cell of a granularity of 0.1x0.1 for Minimum Bias events (right-side) and Pile-Up (left-side) at low luminosity, in 1000 events. On the top, distributions without applied P_T cut for charged particles and on the bottom with the cut off.

8.4 Transverse Energy Deposited by Soft Process

Underlying Events and Minimum Bias are both considered soft process, i.e., these process are characterized by having a very small component of energy in the transverse region, which is the main region of interest for physics analysis.

So although, the occupancy of UE and Pile-Up events (of MB type) is of the same order of the QCDjets, their corresponded energy deposit is much smaller than the QCDjets (Minimum Bias ∼20GeV, Pile-Up ∼45 GeV), even more so if we apply the cut off to the charged hadrons of P_T>0.5 GeV (Minimum Bias ∼7GeV, Pile-Up ∼14 GeV).

It implies that if we applied the Energy Flow algorithm over the E_T deposited by these particles, the influence of the Pile-Up events at low luminosity, could be negligible.

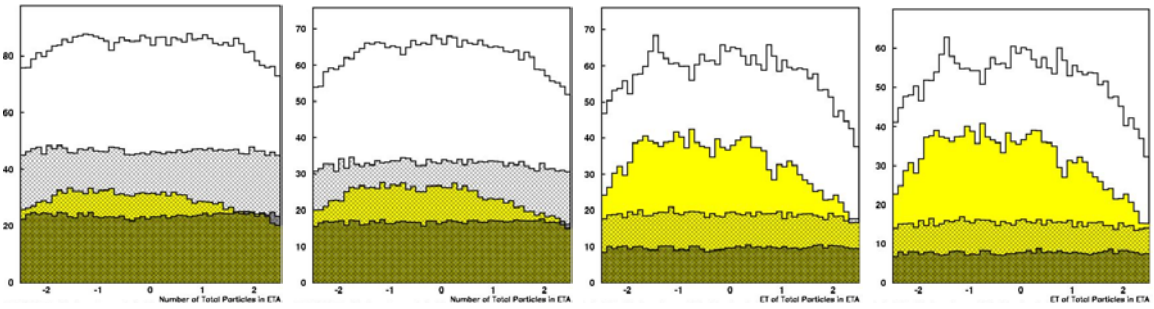

Figure 22: Number of total particles (charged and neutral) and the E_T deposited in each cell, in the 4 cases: QCDJet+Underlying Events, i.e., multiple int on (white histogram), QCDjets only, i.e., multiple int off (yellow histogram), Minimum Bias (grey histogram) and Pile-Up at low luminosity (grid histogram). The first and third plot without P_T cut applied and the second and fourth with it.

8.5 Pile-Up Events at high luminosity

At high luminosity each bunch crossing contains an average of 23 minimum bias events, and if we also take into account the response function of the subdetectors, there are, for example in the Liquid Argon case, 18 bunch crossing each time the detector takes data. So, one pile-up event can consist of almost 500 MB events, although most of them are assigned a small weight though shaping, and finally there are around 40 MB events per bunch crossing.

So in the high luminosity environment, the effect of the Pile-Up events is not negligible respect to the QCDjets signal. We will have a large multiplicity of the tracks and it will be difficult to match correctly to the corresponding charged cluster, which implies the risk of defining in worth way neutral or charged cluster and the impossibility to can apply the Energy Flow Algorithm.

8.6 Application of Energy Flow with Underlying Events

We apply the Energy Flow algorithm to events with Underlying Events. The resolution in energy in the hadronic calorimeter is ∼7.9%. If the parameterization of the inner detector is applied it decreased up to ∼4.9%. So, these results are very similar result to the one obtained without Underlying events.

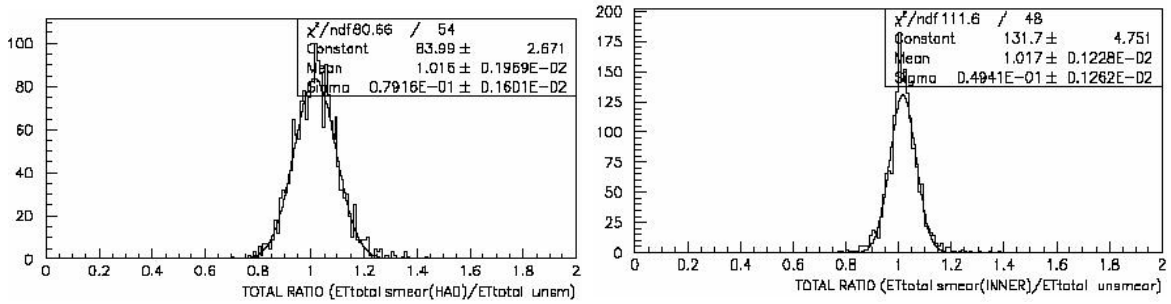

Figure 23: For the range of 40-80 GeV and DR=0.4, the resolution in the E_T of the jet applying Had Calorimeter parameterization is ∼7.9% while if the parameterization of the inner detector is applied the resolution decreased up to ∼4.9%, so the application of the Energy Flow algorithm give an improvement ∼38%

9 Conclusions and further studies

We can conclude that the application of the Energy Flow algorithm at particle level in ATLAS can potentially improve the jets energy resolution. This improvement is better at lower P_T reaching values up to $\sim$40% of relative improvement in the resolution. Nevertheless, around 100 GeV the overlap between particles gets higher and the gain in resolution of the energy jets is marginal.

Respect to the soft process, the influence of the Underlying Events and the Pile-Up events at low luminosity can be negligible for Energy Flow´s resolutions.

However, one should keep in mind that this analysis has been done using a fast simulation package but also a very "simplistic" one, where the effect of the detector and also a lot of circumstances have not been considered.

Atlfast supposes that each particle deposited all its energy in one cell, when in reality particles deposit their energy in a set of cells forming a cluster, whose shape and size depend on multiple factors as the type of particle (EM or HAD shower), the energy, the effect of the magnetic field and the amount of material in front of the calorimeter, which increase the multiplicity from secondary particles (mainly the conversion of photons from π_0) and make wider the cluster. By other hand, Atlfast assumed the corrected match track-cluster, but at high luminosity the multiplicity of the tracks is very large and this is a not simple task.

To take into account all these factors require the use of advanced clustering algorithms capable of efficient isolation of the individual shower together with an energy deposition model. These tools have been actually developed in Full Simulation context[20][21]

So, the particle level study described in this note will be followed up with full simulation studies where the detector response is modelled in a very accurate way by GEANT. Then, realistic study of the energy resolution that can be reached in ATLAS with Energy Flow will be obtained.

In addition, during the summer of 2004 there will be a Combined Test beam where the LArEM calorimeter and the Hadronic Tile Calorimeter will be tested as the same time, as well as the Inner detector. In this combined TB single pions and electrons at very low p_T (from 0.5 to 9 GeV) will be measured, and these will be interesting data to validate Energy Flow algorithm and to understand the influence of the overlap between particles.

References

[1] D. Buskulic et al., (ALEPH Collaboration), *Performance of the ALEPH detector at LEP* CERN-PPE/94-170(1994), Published in: Nucl. Instrum. Methods Phys. Res., **A** 360 (1995) 481-506.
F.Ligabue et al. (ALEPH Collaboration), *Jet Calibration at LEP2*, In Proceedings of the IX Int. Conf in Calorimetry in Part.Phys., CALOR2000, Annecy(2000).

[2] T. Omori et al. (OPAL Collaboration), *Attempt to Compensate Energy in OPAL Calorimeter Complex based on MT Package*, OPAL Technical Note TN-447 (1996).
E. Duchovni et al., (OPAL Collaboration), *GCE++ An Algorithm for Event Energy Reconstruction*, OPAL Technical Note TN-306 (1995).

[3] S. Lami et al., (CDF Collaboration), *Studies of Jet Energy Resolution*, FERMILAB-Conf-00/342-E CDF 2001 (2001).
A. Bhatti et al., (CDF Collaboration), *Review of Jet Clustering at Tevatron*, In Proceedings of the IX Int. Conf in Calorimetry in Part.Phys., CALOR2000, Annecy (2000).
O.Lobban, A. Shiharan and R. Wigmans, (Texas Tech University), *On the Energy measurement of Hadron Jets*, In Proceedings of the X Int. Conf in Calorimetry in Part.Phys., CALOR2002, Pasadena, (2002).

[4] C. Issever et al., (H1 Collaboration), *The calibration of the H1 liquid Argon calorimeter*, In Proceedings of the IX Int. Conf in Calorimetry in Part.Phys., CALOR2000, Annecy, (2000).

[5] J. Breitweg et al., (ZEUS Collaboration), Eur. J. Physics. 1, 81 (1998).
M. Wing (ZEUS Collaboration), *Precise Measurement of the Jet Energies with the ZEUS Detector*, In Proceedings of the IX Int. Conf in Calorimetry in Part.Phys., CALOR2000, Annecy, (2000).

[6] P.Gay, *Energy flow*. In Proceedings of the Linear Collider Workshop 2000, Fermilab, Batavia, IL, USA, 2000. http://www-lc.fnal.gov/lcws2000
V.L. Morgunov *Calorimetry Design with Energy-Flow concept (Imaging Detector for High-energy Physics)*, In Proceedings of the X Int. Conf in Calorimetry in Part.Phys., CALOR2002, Pasadena, (2002).

[7] D. Green *Energy Flow in CMS Calorimetry* Fermilab-FN-0709
S. Kunori (CMS Collaboration), *Jet Energy Reconstruction with the CMS Detector*, In Proceedings of the X Int. Conf in Calorimetry in Part.Phys., CALOR2002 Conference, Pasadena, (2002).
D.Green et al., *Energy flow objects and usage of tracks for energy measurement in CMS*, CMS NOTE 2002/036, Sept (2002).

[8] M. Wierlers (ATLAS Collaboration), *Performance of Jets and missing ET in ATLAS*, talk at CALOR2002 Conference, Pasadena, (2002).

[9] eflowRec package: Energy Flow Reconstruction in Athena (Dan Tovey) http://atlas.web.cern.ch/Atlas/GROUPS/PHYSICS/JETS/EFLOWREC/eflowrec.htm

[10] C. Iglesias, *Reconstruccion de Jets mediante el algoritmo Energy Flow en ATLAS*, talk in VII Jornadas de Fisica de Altas Energia, XXIX Reunion Bienal, Madrid, (2003).

[11] R. Wigmans, *Calorimetry - Energy Measurement in Particle Physics*, Internal Series of monographs on Physics, vol 107, Oxford University Press (2000).

[12] ATLAS Collaboration, ATLAS Detector and Physics Performance Technical Design Report CERN/LHCC/99-14, ATLAS TDR 14 (1999).

[13] C++ version of Atlfast in Athena, http://www.hep.ucl.ac.uk/atlas/atlfast

[14] E.Richter-Was, 'ATLFAST 2.0 A fast simulation package for ATLAS', ATLAS Note ATL-PHYS-98-131 (1998)

[15] Athena User and Developer Guide v.2.0 & Releases http://atlas.web.cern.ch/Atlas/GROUPS/SOFTWARE/OO/architecture/General/

[16] Geant4 Users documents: http://wwwasd.web.cern.ch/wwwasd/geant4/G4UsersDocuments/Overview/html/index.html

[17] T.Sjostrand, Comput. Phys. Commun. **82** (1994):, T.Sjostrand et al, Comput. Phys. Commun. **135** (2001) 238; T.Sjostrand, L. Lonnblad and S Mrenna PYTHIA 6.2 - Physics and Manual, [online] hep-ph/0108264, august:2001. Available from: http://weblib.cern.ch/.

[18] ATLAS Calorimeter Performance, CERN/LHCC/96-40, ATLAS TDR 1, (1996).

[19] A.Moraes, I.Dawson, C. Buttar. Comparison of predictions for minimum bias event generator and consequences for ATLAS radiation background. ATL-PHYS-2003-020 (2003)
Minimum bias and the underlying event: ATLAS tuning presented by A. Moraes at the Workshop on Monte Carlo tools for the LHC - CERN; 31st Jul 2003.

[20] S.Menke talks: Status of Topological Clustering,, Software Performance Meeting, LAr Week (CERN), 28. Jan 2004 and Status of Topological Clustering recent Reco-Software Changes, Hadronic Calibration meeting (CERN), 13 May 2004.

[21] C.Iglesias IFIC talks: TiCal-IFIC Weekly Meetings (Valencia, SPAIN)
C.Iglesias, Clustering of very low ET particles, Software Workshop, Reconstruction Working Group: Calorimetry, Sep,2004, CERN
C.Iglesias, Clustering of very low ET particles, ATLAS communication in preparation.

C.Iglesias, Clustering of very low ET particles in Combined TB, ATLAS Calorimetry Calibration Workshop, Hadronic Calibration Session, Dec 2004, Trata, Slokavia